Eur Biophys J (2004) 33: 377–385
DOI 10.1007/s00249-003-0369-9

ARTICLE

**Jakub Włodarczyk · Gerasim Stoychev Galitonov
Borys Kierdaszuk**

Identification of the tautomeric form of formycin A in its complex with *Escherichia coli* purine nucleoside phosphorylase based on the effect of enzyme–ligand binding on fluorescence and phosphorescence

Received: 21 July 2003 / Revised: 21 July 2003 / Accepted: 15 October 2003 / Published online: 4 December 2003

Abstract Fluorescence and phosphorescence emission spectroscopy were employed to study the interaction of *Escherichia coli* purine nucleoside phosphorylase (PNP) with its specific inhibitor, formycin A (FA), a close structural analogue of adenosine (natural substrate), in the absence and presence of phosphate (P_i, substrate). Formation of enzyme–FA complexes led to marked quenching of enzyme tyrosine intrinsic fluorescence and phosphorescence, with concomitant increases in fluorescence and phosphorescence of FA. Fluorescence resonance energy transfer from the protein Tyr160 residue to the FA base moiety was identified as a major mechanism of protein fluorescence quenching, increased by addition of P_i. The effects of enzyme–FA interactions on the nucleoside excitation and emission spectra for fluorescence and phosphorescence revealed shifts in the tautomeric equilibrium of the bound FA, i.e. from the N(1)–H tautomer (predominant in solution) to the N(2)–H form, enhanced by the presence of P_i. The latter was confirmed by enzyme–ligand dissociation constant (K_d) values of 5.9 ± 0.4 and 2.1 ± 0.3 μM in the absence and presence of P_i, respectively. Addition of glycerol (80%, v/v) led to a lower enzyme affinity ($K_d \approx 70$ μM), without changes in binding stoichiometry. Enzyme–FA complex formation led to a higher increase of the fluorescence than the phosphorescence band of the ligand, consistent with the fact that the N(2)–H tautomer is characterized by a weaker phosphorescence than the N(1)–H tautomeric form. These results show, for the first time, the application of phosphorescence spectroscopy to the identification of the tautomeric form of the inhibitor bound by the enzyme.

J. Włodarczyk · G. Stoychev Galitonov · B. Kierdaszuk (✉)
Institute of Experimental Physics,
Department of Biophysics,
University of Warsaw,
93 Żwirkii Wigury Street,
02-089 Warsaw, Poland
E-mail: borys@biogeo.uw.edu.pl
Fax: +48-22-5540771

Keywords Enzyme–ligand binding · Fluorescence and phosphorescence · Formycin A · Purine nucleoside phosphorylase · Tautomerism

Abbreviations Ado: adenosine · FA: formycin A [3-(β-D-ribofuranosyl)-7-aminopyrazolo[4,3-*d*]pyrimidine] · FB: formycin B · FRET: fluorescence resonance energy transfer · Guo: guanosine · Hepes: *N*-(2-hydroxyethyl)piperazine-*N*′-(2-ethanesulfonic acid) · Ino: inosine · m^1FA: *N*(1)-methylformycin A · m^2FA: *N*(2)-methylformycin A · m^4FA: *N*(4)-methylformycin A · m^6FA: *N*(6)-methylformycin A · m^7Guo: *N*(7)-methylguanosine · P_i: orthophosphate · PNP: purine nucleoside phosphorylase · Xao: xanthosine

Introduction

The ubiquitous purine nucleoside phosphorylase (PNP, purine nucleoside:orthophosphate ribosyl transferase, EC 2.4.2.1.) catalyzes the reversible cleavage of the glycosidic bond of (2′-deoxy)ribonucleosides of guanine and hypoxanthine in higher organisms, as well as of adenine in some prokaryotes, e.g. *Escherichia coli* and *Salmonella typhimurium*, as follows:

$$\beta\text{-nucleoside} + P_i \rightleftarrows \text{purine base} + \alpha\text{-D-pentose-1-phosphate} \quad (1)$$

It is worth noting that some organisms like *E. coli* code for two forms of PNPs. One, a product of the *xapA* gene (Buxton et al. 1980; Hammer-Jespersen et al. 1980), sometimes called inosine-xanthosine phosphorylase, is active towards guanosine (Guo), inosine (Ino) and xanthosine (Xao) (Bezirjian et al. 1986; Koszalka et al. 1988), but inactive with adenosine (Ado). In contrast, the product of the *deoD* gene (Jensen and Nygard 1975; Jensen 1976; Doskocil and Holy 1977), which is studied here, is inactive against Xao, but exhibited activity towards Ado, like PNPs from many prokaryotes, e.g. *S. typhimurium* (Jensen and Nygard 1975; Jensen 1976).

PNP is recognized as a primary target for immunosuppressive agents (Kredich and Hershfield 1989; Gilbertsen and Sircar 1990) in organ transplantation and autoimmune diseases such as lupus or rheumatoid arthritis (Stoeckler et al. 1980). PNP inhibitors are also promising drugs for prevention of intracellular phosphorolytic cleavage of therapeutically active nucleoside analogues. It is therefore not surprising that widespread attention is directed to studies on the mechanism of action of this enzyme from various sources, and searches for more potent inhibitors (Stoeckler 1984; Montgomery 1993; Bzowska et al. 2000; Pugmire and Ealick 2002). One of the most important applications of bacterial PNP is in tumour-directed gene therapy (Sorscher et al. 1994; Hughes et al. 1995), based on the much broader substrate specificity of PNP from *E. coli* (Doskocil and Holy 1977) compared to that from human erythrocytes (Stoeckler 1984).

Formycin A (FA) and formycin B (FB), close structural analogues of Ado and Ino (but with a non-cleavable C–C glycosidic bond, see Scheme 1), are good competitive inhibitors of the *E. coli* enzyme (Bzowska et al. 1992), with K_i values of ~5 μM versus Ino. *N*(6)-Methylformycin A (m^6FA), a structural analogue of *N*(1)-methyladenosine, exhibits very good inhibitory activity, with $K_i = 0.3$ μM. In contrast, FA and m^6FA are totally inactive, and FB exhibits poor affinity ($K_i \approx 100$ μM) versus the enzymes from calf spleen and human erythrocytes. In order to explain their good inhibitory activity versus the *E. coli* enzyme, X-ray crystallographic studies were performed and led to the 3-D structure of the ternary complex of *E. coli* PNP with FB and P_i (Koellner et al. 1998), and with m^6FA and P_i (Koellner et al. 2002). Since X-ray crystallography is not able to determine the position of hydrogen atoms, unequivocal identification of the tautomeric forms of FB and m^6FA in the complexes was not possible. This has prompted extensive studies with the aid of static and time-resolved fluorescence spectroscopy (Kierdaszuk et al. 2000; Kierdaszuk 2002), and revealed that complex formation with the enzyme leads to a tautomeric shift for both FA and FB in favour of the *N*(2)–H tautomeric form, i.e. the minor form of the free ligands in aqueous solution.

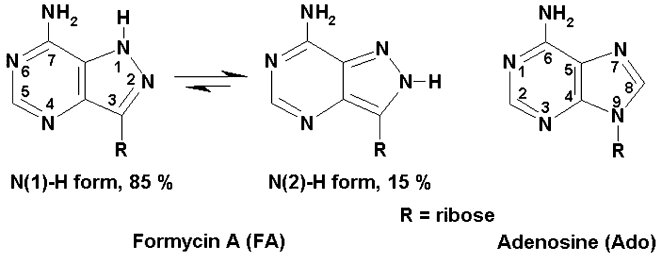

Scheme 1 The structurally similar neutral forms of formycin A and adenosine (R = ribose). Formycin A consists of an equilibrium mixture of two tautomeric species, N(1)–H and N(2)–H, in the proportions indicated. Note the close structural resemblance of the tautomeric species to the fixed tautomeric forms of formycin A, i.e. *N*(1)-methyl and *N*(2)-methyl analogues of formycin A, respectively. Note also the different numbering systems for the two rings, according to IUPAC

Particularly interesting are the structural requirements of the enzyme towards tautomeric forms of inhibitors (Kierdaszuk 2002) observed in the case of FA and m^6FA (Kierdaszuk et al. 2000), and the P_i dependence of the latter. In the presence of 1 μM (background) P_i, i.e. with no extra P_i added, the imino form of m^6FA was selectively bound by the enzyme, albeit with low affinity ($K_d = 46$ μM), while addition of 20 mM P_i changed the preferential binding towards the amino form of m^6FA (Kierdaszuk et al. 2000) with much higher enzyme–ligand affinity ($K_d = 0.5$ μM). This is in contrast to bisubstrate analogue inhibitors (Halazy et al. 1991), e.g. acyclovir diphosphate (Tuttle and Krenitsky 1984; Krenitsky et al. 1990), where addition of phosphate leads to lower enzyme–inhibitor affinity. Dependence of the inhibitory activity of the latter on phosphate is not surprising, because it simultaneously interacts with the binding sites for both nucleoside and phosphate. Thus, PNP affinity for inhibitors is markedly dependent on the P_i concentration, and reflects the existence of two states of the enzyme with different affinities for P_i (Kierdaszuk et al. 1997).

It has long been known that FA and some *N*-methylated analogues are phosphorescent, with good quantum yields (Ward et al. 1969; Wierzchowski and Shugar 1982). We herein describe the use of phosphoresce emission spectroscopy to study the interactions of FA with *E. coli* PNP in the absence and presence of P_i, which leads to identification of the tautomeric form of FA bound by the enzyme, and provides complementary data versus enzyme–nucleoside binding deduced from X-ray structural studies in the solid state, where unequivocal determination of tautomeric forms is not possible.

Materials and methods

Formycin A (FA), inosine (Ino), *N*-(2-hydroxyethyl)piperazine-*N*′-(2-ethanesulfonic acid) (Hepes), mono- and dibasic sodium phosphates, and xanthine oxidase from buttermilk (grade III, 1 U/mg) were from Sigma (St. Louis, Mo., USA). Glycerol was from Fluka (Switzerland).

All solutions were prepared with high-quality MilliQ water. Reagents were of the highest quality commercially available, and only those of spectral grade, checked by UV absorption and/or fluorescence emission, were employed.

Concentrations of substrates and inhibitors were determined spectrophotometrically at pH 7.0 for: FA, $\lambda_{max} = 294$ nm ($\epsilon = 10.3 \times 10^3$) (Giziewicz and Shugar 1977; Wierzchowski et al. 1980); Ino, $\lambda_{max} = 248$ nm ($\epsilon = 12.3 \times 10^3$) (Dawson et al. 1969; Lister 1971; Psoda and Shugar 1971); and PNP, $\lambda_{max} = 277$ nm ($\epsilon = 43 \times 10^3$) (Kierdaszuk et al. 2000).

Ultraviolet absorption was monitored with a Kontron (Switzerland) UVIKON 922 recording instrument fitted with a thermostatically controlled cell compartment, using 2-, 5- and 10-mm pathlength cuvettes. Measurements of pH (±0.05) were with a CP315m (Elmetron, Poland) pH-meter equipped with a combination semi-micro electrode (Orion, UK) and temperature sensor.

Partially purified PNP from *E. coli* (~60% pure, about 60 U mg^{-1}), a gift of Dr G. Koszalka (Wellcome Research Labs, Research Triangle Park, NC, USA) was further purified to

apparent homogeneity and final specific activity 105 U mg^{-1} (Kierdaszuk et al. 1997). The enzyme consists of six identical subunits, and enzyme concentrations are expressed in terms of the native hexamer, unless otherwise stated.

Enzyme activity was monitored at 25 °C in 50 mM phosphate buffer (pH 7.0) spectrophotometrically by the coupled xanthine oxidase procedure with Ino as substrate (Kalckar 1947; Stoeckler et al. 1978).

Steady-state fluorescence measurements

Steady-state fluorescence spectra were monitored at 180 and 300 K on a Spex (USA) FluoroMax spectrofluorimeter with 2-nm spectral resolution for excitation and emission. Steady-state phosphorescence spectra were recorded on a home-made phosphorimeter (Parker 1968) with detection of photons based on time-correlated single-photon counting electronics. Samples were thermostated using a home-made liquid nitrogen cryostat (Institute of Physics, Polish Academy of Sciences, Warsaw). The temperature was measured directly in the solution by a diode thermometer, with an accuracy of 0.5 K. Enzyme samples (0.5–2 μM) were prepared in 500 μL of 50 mM Hepes (pH 7.0) in the absence or presence of glycerol (80%, v/v) in 5×5-mm Suprasil cuvettes.

Hepes was selected to avoid buffer effects, previously noted with Tris and other buffers (Wierzchowski et al. 1996; Stoychev et al. 2001), although overlooked in most reports. Solutions contained background contaminant phosphate, 1 μM, estimated spectrophotometrically (Ames 1966), sufficiently low so as not to affect the overall results and conclusions, and these solutions are referred to as controls free of P_i.

The fluorescence of protein, nucleosides and their mixtures was excited at several wavelengths in the range 260–320 nm, and fluorescence and/or phosphorescence spectra recorded in the range 290–450 nm and/or 350–550 nm, respectively. For quenching studies, additions to the enzyme were made from FA stock solutions prepared in the same buffer and at the same pH as the enzyme sample, and changes in fluorescence were usually monitored at several wavelengths with $\lambda_{exc} = 270$, 295, 305 and 320 nm. Emission and excitation spectra were recorded prior to, and during, titration. Dilution did not exceeded 10%, and the fluorescence intensity was corrected for the dilution factor. Background emission (< 5%) was eliminated by subtracting the signal for buffer and/or buffer containing the appropriate quantity of ligand. The total absorbency of the enzyme–ligand mixtures did not exceed 0.2 to minimize inner-filter effects. To compensate for the decrease in fluorescence due to increased absorption, the measured fluorescence was multiplied by a correction factor, $G(\Delta A_1, \Delta A_2) = \text{anti-log}_{10}[(\Delta A_1 + \Delta A_2)/2]$, where ΔA_1 and ΔA_2 are the increases in absorption at the excitation and emission wavelengths when the ligand was added (Lakowicz 1999). Enzyme activity was not affected by titration, nor by freezing during formation of water/glycerol glassy solutions, as checked by activity measurements before and after the experiments.

Ligand binding

Ligand binding led to only partial quenching of the protein fluorescence, with virtually no modification of the emission spectrum (see section on Fluorescence and phosphorescence properties of *E. coli* PNP and FA). To obtain dissociation constants (K_d) for enzyme–ligand binding, and binding stoichiometry for the ligands, a simple two-state association $E + L \rightleftharpoons EL$ was considered using a model of identical and non-interacting sites (Eftink 1997). Note that a two-state equilibrium between bound and free ligand is reflected in the existence of isoemissive points in fluorescence–emission difference spectra, e.g. at 307 nm (Fig. 2A) and 309 nm (Fig. 2B), and in fluorescence–excitation difference spectra at ~295 nm (Fig. 2, insets), lending added confidence to the accuracy of the measurements. This led to a set of equations with unknown values (K_d, [E], [L], [EL], f_E, f_L, f_{EL}): $K_d = [L][E]/[EL]$, $[L_0] = [L] + [EL]$, $[E_0] = [E] + [EL]$, $F = [E]f_E + [EL]f_{EL} + [L]f_L$ and $F_0 = [E_0]f_E$, where F_0 and F are the fluorescence intensities in the absence and presence of a quenching ligand (quencher); $[E_0]$ is the effective concentration of binding sites; $[L_0]$ is the total concentration of ligand; [E] is the molar concentration of free binding sites; [L] and [EL] are the molar concentrations of free ligand and enzyme–ligand complexes, respectively; K_d is the dissociation constant of the latter; f_E, f_L and f_{EL} are the fluorescence coefficients of free enzyme, free ligand and enzyme–ligand complexes, respectively. Solving this set of equations results in:

$$F = F_0 + [L_0]f_L + 0.5f_p\left([L_0] + [E_0] + K_d - \sqrt{([L_0] + [E_0] + K_d)^2 - 4[L_0][E_0]}\right) \quad (2)$$

where $f_P = f_{EL} - f_E - f_L$, and K_d and f_P were fitted non-linearly, assuming binding of one, two, three or six ligand molecules per native enzyme hexamer, i.e. $[E_0]$ equal to single-, two-, three- or six-fold enzyme concentration. Equation (2) was fitted using non-linear regression analysis. The χ^2 values and residuals — the differences, and/or relative differences, between calculated and experimental values — were used to test the quality of the fits.

Fluorescence resonance energy transfer

Tyrosine fluorescence of *E. coli* PNP (donor) is overlapped by the absorption of FA (acceptor) (Fig. 1); hence the Förster radius (R_0) for this donor–acceptor pair can be calculated as described elsewhere for other analogous systems (Förster 1948; Wu and Brand 1994):

$$R_0 = 9.7 \times 10^3 \left(J\kappa^2 n^{-4} \phi_D\right)^{1/6} \quad (3)$$

where:

$$J = \int \varepsilon_A(v) f_D(v) v^{-4} dv \quad (4)$$

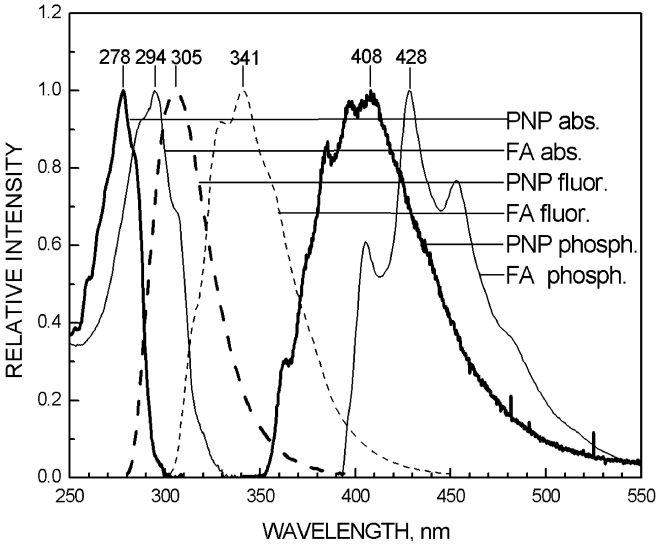

Fig. 1 UV absorption (*abs.*) and fluorescence (*fluor.*) and phosphorescence (*phosph.*) spectra of 1 μM PNP from *E. coli* and the neutral form of 25 μM FA in 50 mM Hepes (pH 7) (absorption and fluorescence, at 298 K) and 50 mM Hepes (pH 7) containing 80% glycerol (phosphorescence, at 180 K). Maximum intensities of the absorption and emission spectra of PNP ($\lambda_{exc} = 270$ nm) and FA ($\lambda_{exc} = 295$ nm) are normalized to unity

J is a measure of the spectral overlap between emission of the donor and absorption of the acceptor; f_D and ε_A are the normalized fluorescence spectrum of the donor and absorption spectrum of acceptor, respectively; n is the refractive index of the medium between donor and acceptor (taken as 1.4 for aqueous solution); ϕ_D is the quantum yield of the donor in the absence of the acceptor (0.067 for $\lambda_{exc} = 270$ nm); and κ^2 is the orientation factor, replaced here by its spatial average ($<\kappa^2> = 2/3$) over all donor and acceptor orientations.

Results and discussion

Fluorescence and phosphorescence properties of *E. coli* PNP and FA

The maxima of the absorption, fluorescence and phosphorescence emission spectra of PNP are located at 277, 304 and 408 nm, respectively (Fig. 1), consistent with the fact that each of the subunits of the *E. coli* enzyme contains six tyrosine residues and no tryptophan (Hirshfield et al. 1991). By contrast, FA (Scheme 1) exhibits absorption ($\lambda_{max} = 294$ nm) and emission spectra red-shifted ($\lambda_{max} = 341$ and 428 nm for fluorescence and phosphorescence) relative to the spectra for PNP (Fig. 1, Table 1). This permits selective excitation of the ligand in the enzyme–ligand complexes at excitation wavelengths above 295 nm, where tyrosine residues do not absorb. Selective observation of PNP fluorescence and phosphorescence is possible in the range 290–310 nm and 350–390 nm, respectively, while fluorescence and phosphorescence of the ligand occur at wavelengths above 360 and 430 nm, where contributions of the respective protein emissions are usually negligible (Fig. 1).

Effect of enzyme–FA interaction on fluorescence

Addition of increasing concentrations of FA to the solution of PNP in 50 mM Hepes (pH 7) containing 80% glycerol led to a partial quenching of enzyme tyrosine fluorescence ($\lambda_{em} = 304$ nm) without affecting the location of the maxima for excitation (absorption) or emission of the enzyme. Concomitantly, the decrease in enzyme emission was accompanied by an increase in emission of FA at 341 nm (Fig. 2A and 2B) due to the enzyme–ligand fluorescence resonance energy transfer (FRET) (Kierdaszuk et al. 2000), confirmed by fluorescence excitation spectra (Fig. 2A and 2B, insets). The well-defined vibrational structure, particularly visible in the fluorescence–emission difference spectra at excitation to the red of 295 nm (Fig. 3), where protein tyrosine residues do not absorb (Fig. 1), is red-shifted relative to the fluorescence emission of free FA, and better resembles the emission bands of the N(2)–H than the N(1)–H tautomer of FA (Wierzchowski and Shugar 1982). The latter is further confirmed by the pronounced enhancement of the excitation bands at 308 and 320 nm in the fluorescence–excitation difference spectra ($\lambda_{em} = 365$) by increasing concentrations of FA (Fig. 2, insets). All the foregoing are consistent with the fact that both excitation and emission spectra of the N(2)–H form of FA are red-shifted relative to that of the N(1)–H form (Wierzchowski and Shugar 1982; Kierdaszuk 2002), as shown for the excitation and emission spectra of m^2FA and m^1FA (Table 1), which are good models of the fixed N(2)–H and N(1)–H tautomers of FA (Wierzchowski and Shugar 1982), respectively. Additionally, the increasing intensity of the band at 277 nm in the excitation spectrum shows FRET between tyrosine residue(s) of the enzyme and the N(2)–H from of FA (see below).

Particularly important are the isoemissive points, in both fluorescence–emission difference spectra ($\lambda_{em} = 307$ and 309 nm in Fig. 2A and 2B) and fluorescence–excitation difference spectra ($\lambda_{exc} = 295$ nm in Fig. 2, insets). They testify the existence of a two-state equilibrium between bound and unbound ligand, which, in fact, may by properly described by Eq. (2). These enable characterization of the enzyme–ligand interactions by titration

Table 1 UV absorption properties of *Escherichia coli* PNP, FA and the neutral forms of its analogues (m^1FA, m^2FA) in 50 mM Hepes buffer (pH 7.0) at 298 K, and their fluorescence and phosphorescence properties in 50 mM Hepes buffer (pH 7.0) containing 80% glycerol at 180 K

Compound	pK_{a1}	pK_{a2}	Absorption[a]		Fluorescence		Phosphorescence	
			λ_{max} (nm)	$\epsilon_{max}\times10^{-3}$($M^{-1}$ cm^{-1})	λ_{exc} (nm)	λ_{max} (nm)	λ_{exc} (nm)	λ_{max} (nm)
PNP			277	43.2[b]	–[c]	304	–[c]	408
FA	4.3	9.7	294	10.3				
					294	338	294	428
					320	352		
m^1FA	4.0		302	10.0				
			232	7.7				
					–[c]	347	–[c]	442
m^2FA	4.9		306	11.0				
			234	5.2				
					–[c]	353	–[c]	470

[a]UV absorption properties were described previously for *E. coli* PNP (Kierdaszuk et al. 2000) and for FA, m^1FA and m^2FA (Giziewicz and Shugar 1977; Wierzchowski et al. 1980)
[b]Molar extinction coefficient for native hexamer based on Kierdaszuk et al. (2000)
[c]Values independent of λ_{exc}

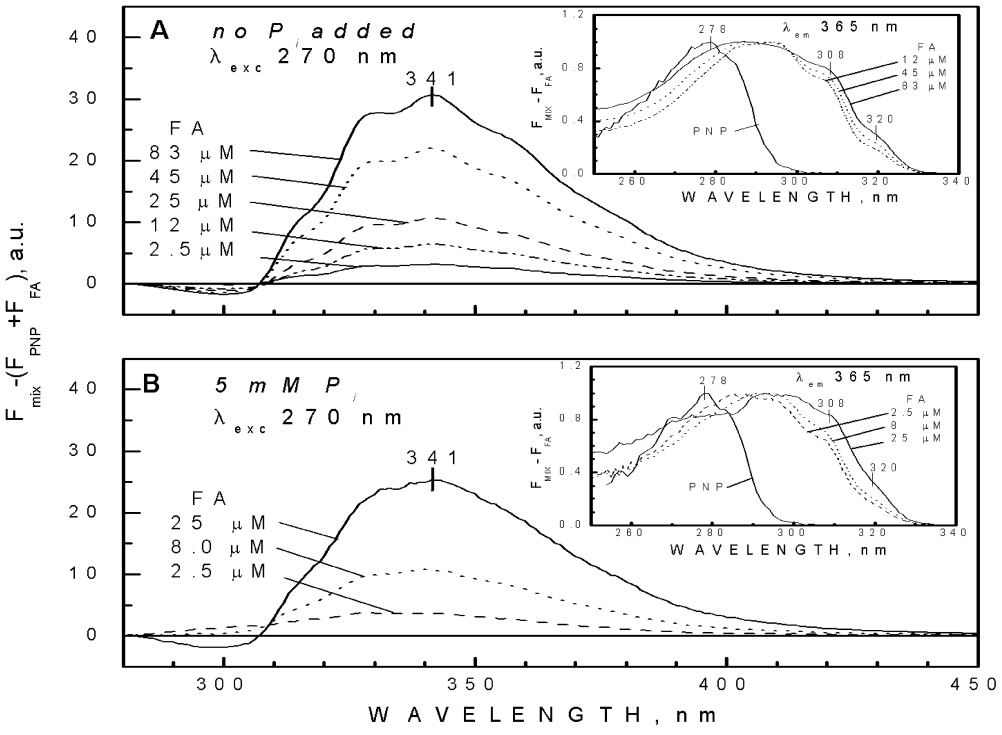

Fig. 2 Fluorescence–emission difference spectra ($\lambda_{exc} = 270$ nm) of 1 μM PNP + increasing concentrations of FA, relative to the arithmetic sum of the two components, in 50 mM Hepes (phosphate-free) buffer (pH 7) containing 80% glycerol at 300 K: (**A**) in the absence and (**B**) in the presence of 5 mM P_i. The *insets* show the fluorescence excitation difference spectra ($\lambda_{em} = 365$ nm) of a mixture of 1 μM PNP + increasing concentrations of FA, relative to the excitation spectra of FA, in the absence (**A**) and presence (**B**) of 5 mM P_i, respectively. Note the isoemissive points in this (and subsequent) figures, testifying to a two-state equilibrium between free and bound ligand

of the emission of the enzyme and/or ligand (inhibitor) as a function of ligand concentration. Fitting the data, by non-linear regression, to different models for enzyme–ligand binding (Eftink 1997) gave the best fit for a model with binding of one ligand per native enzyme hexamer (Eq. 2), with dissociation constant (K_d) values listed in Table 2. The resulting K_d values showed that, in the absence of glycerol, addition of P_i led to much higher affinity for the enzyme, i.e. in the presence of P_i, K_d is three-fold lower than in the absence of P_i. Addition of 80% glycerol led to a much lower enzyme–FA affinity characterized by at least one range of higher K_d values,

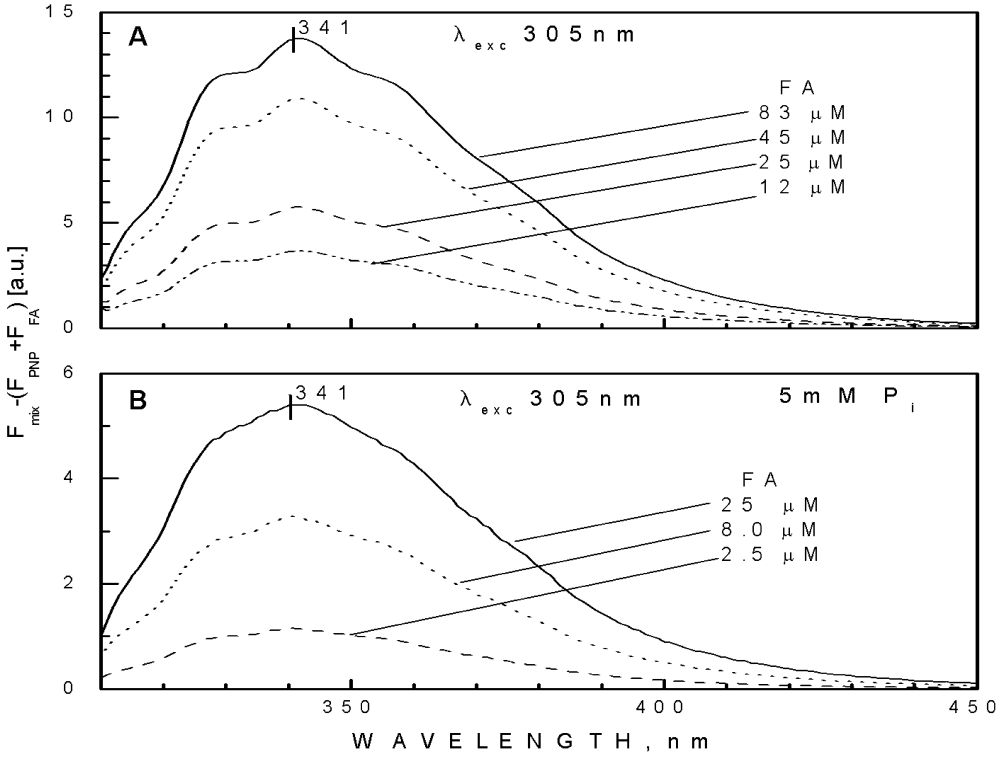

Fig. 3 Fluorescence–emission difference spectra ($\lambda_{exc} = 305$ nm) of 1 μM PNP + increasing concentrations of FA, relative to the arithmetic sum of the two components, in 50 mM Hepes (phosphate-free) buffer (pH 7) containing 80% glycerol at 300 K, in the absence (**A**) and presence (**B**) of 5 mM P_i

Table 2 Dissociation constants (K_d) of FA binding to the native enzyme hexamer calculated from non-linear fits of a model of six independent and non-interacting sites (Eq. 2) to the steady-state quenching of PNP fluorescence at 300 nm ($\lambda_{exc} = 260$ nm) by increasing concentrations of FA in 50 mM Hepes (pH 7) in the absence and presence of phosphate (P_i) and/or 80% (v/v) glycerol

Orthophosphate (mM)	K_d (μM)	
	0% glycerol	80% glycerol
≤ 0.001	5.9 ± 0.4	70 ± 2
5.0	2.1 ± 0.3	72 ± 4

independently of P_i (Table 2). Comparison of the values for K_d with those for K_i for inhibition of the enzyme by FA (Bzowska et al. 1992) may be only qualitative, because different conditions are necessarily required for measurements of K_i, e.g. the use of a broad range of substrate concentrations and an obligatory presence of P_i (substrate). Additionally, K_i values are often dependent on P_i concentration (Halazy et al. 1991), and the effect of glycerol on K_d cannot be fully explained at this moment. It may reduce the PNP–FA affinity by its effect on the network of hydrogen bonds formed by three water molecules between the N(1) and N(6) atoms of the ligand base moiety and the carboxylic group of Asp204, observed in the solid-state structure of the enzyme with both FB (Koellner et al. 1998) and m^6FA (Koellner et al. 2002).

As was indicated previously (Kierdaszuk et al. 2000), singlet–singlet energy transfer plays a major role in the PNP fluorescence quenching by FA. Analysis of the spectral properties of protein, ligand and enzyme–ligand mixtures pointed to the protein tyrosine residue(s) as donor(s), and to the base moiety of FA as acceptor. The existence of FRET is consistent with good alignment of the respective spectral bands of the donor emission and acceptor absorption (Fig. 1). The Förster radius (R_0) for tyrosine residue(s) and FA participating in the transfer was calculated (Eq. 3) and gave a value of 7 Å, pointing to Tyr160 as the most probable energy donor. This is consistent with the data obtained from examination of the crystal structure of the complex of *E. coli* PNP with FB (Koellner et al. 1998) and with m^6FA (Kolellner et al. 2002), where the planar base moieties of FA and m^6FA are parallel to the phenol residue of Tyr160, and the distances between the middle point of the base rings of FB or m^6FA and the phenol ring of Tyr160 are about 10 Å, three-fold higher then the van der Waals distances between them. Crystal data show that the base moieties of both FB and m^6FA, and the phenol ring of Tyr160, are involved in π–π interactions with the aromatic residue of Phe159, which is located between them almost perpendicular to the base moieties of FB or m^6FA from one side and to the phenol ring of Tyr160 on the other side. Although direct π–π interactions between FA and Tyr160 are weaker than that at their van der Waals contact, approximation of the resonance interaction by a weak coupling between transition dipoles of emission and absorption of Tyr160 and FA (Förster model) is not applicable, and the resulting R_0 value must be considered as a rough estimation. Such π–π stacking implies involvement of higher order multipole couplings as well as exchange interactions. The latter can be ascertained from the transfer rates (Lakowicz 1999), which are usually larger than that calculated from the Förster model, and suggest application of time-resolved techniques. Studies on time-resolved fluorescence intensity and anisotropy decays are presently being attempted.

Effect of enzyme–FA interaction on phosphorescence

Application of phosphorescence spectroscopy to the study of PNP–FA interactions is based on the observation made two decades ago (Wierzchowski and Shugar 1982) that the phosphorescence band of m^2FA is much weaker relative to its fluorescence band than that of m^1FA, which are models for the fixed N(2)–H and N(1)–H tautomers of FA. Indeed, addition of FA to PNP in aqueous/glycerol glassy solution at 180 K led to a relatively weaker phosphorescence than fluorescence emission at $\lambda_{exc} = 294$ nm (Fig. 4A), further enhanced in the presence of a saturating (5 mM, see Kierdaszuk et al. 1997) concentration of P_i (Fig. 4B). When the excitation was moved to 320 nm, where absorption is dominated by the N(2)–H tautomer of FA (Wierzchowski and Shugar 1982; Kierdaszuk 2002), and tyrosine residues in protein do not absorb at all (Fig. 1), the phosphorescence band of the enzyme–ligand mixture is barely visible (Fig. 4A and 4B), independently of P_i. Furthermore, fluorescence excitation spectra ($\lambda_{em} = 338$ nm) of the enzyme–FA complex in the same medium (Fig. 4A, inset) further confirm that the N(2)–H tautomer of FA is bound by the enzyme (Kierdaszuk et al. 2000). This leads to a shift of the tautomeric equilibrium of FA, which exists predominantly as the N(1)–H tautomeric form in solution (Chenon et al. 1976), to the N(2)–H form. The latter is also reflected by an increase of excitation (absorption) intensity at 308 and 320 nm (Fig. 4A, inset). Moreover, an increase in the fluorescence excitation spectra of the enzyme–ligand mixture in the range 260–290 nm showed FRET between tyrosine residues of PNP and the FA ligand in aqueous/glycerol solution (see previous subsection), similar to that observed previously in aqueous medium (Kierdaszuk et al. 2000)

In accordance with the foregoing, a clear-cut correlation was observed between the effects of P_i on the fluorescence and phosphorescence spectra of the PNP–FA complex (Fig. 5A) and a shift in the tautomeric equilibrium of FA. Addition of 5 mM P_i led to an increase in fluorescence intensity in the range 350–390 nm, where emission is dominated by the N(2)–H tautomeric form of FA (Kierdaszuk et al. 2000), and a concomitant decrease of the phosphorescence intensity in the range 410–500 nm due to an increasing population of the N(2)–H tautomeric form. The latter is confirmed by a relative decrease of intensity in the phosphorescence

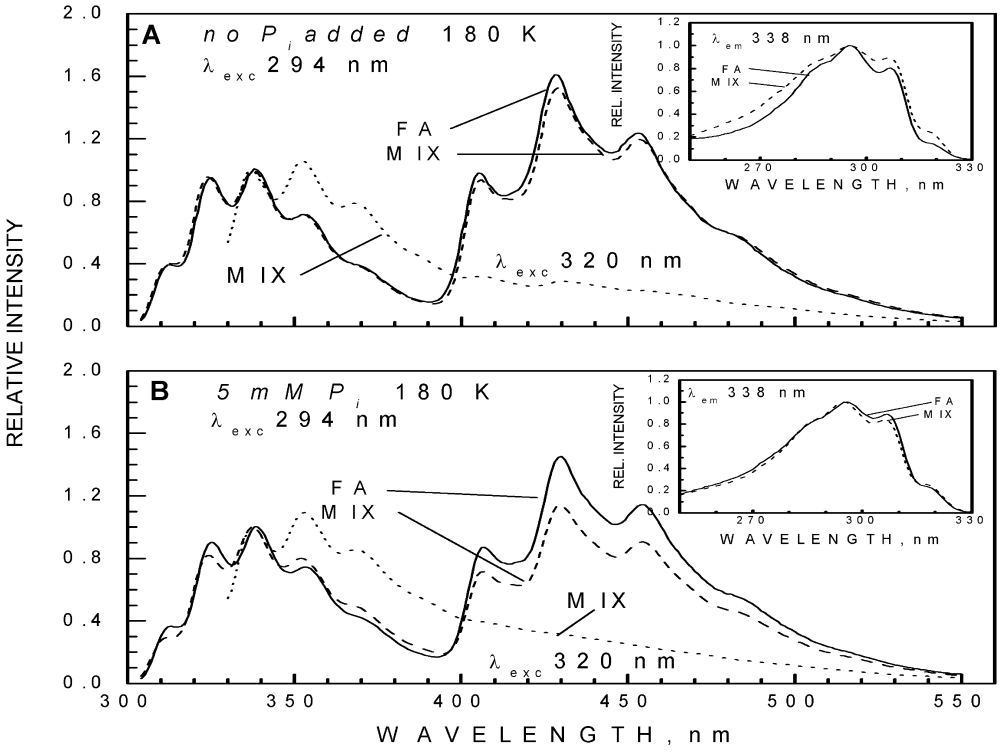

Fig. 4 Fluorescence and phosphorescence emission spectra of 25 μM FA at $\lambda_{exc} = 294$ nm (*full line*) and its mixture with 1 μM PNP at $\lambda_{exc} = 294$ nm (*dashed line*) and $\lambda_{exc} = 320$ nm (*dotted line*), in 50 mM Hepes (phosphate-free) buffer (pH 7) containing 80% glycerol at 180 K, in the absence (**A**) and presence (**B**) of 5 mM P_i. The *insets* show the fluorescence excitation spectra ($\lambda_{em} = 338$ nm) of the same samples. Maximum intensities of the fluorescence emission are normalized to unity

excitation spectra ($\lambda_{em} = 440$ nm) at 308 nm (Fig. 5B, inset). It is worth noting that P_i effects on the emission spectra of the enzyme–FA complex are much stronger than those in the case of free FA in the same medium (Fig. 5B). The foregoing results are consistent with an increase in the population of the N(2)–H tautomeric form of FA due to enzyme–FA binding.

Conclusions

The overall results presented above demonstrate the marked effects of interaction between *E. coli* PNP and its specific inhibitor FA on the emission and excitation spectra for fluorescence and phosphorescence of the

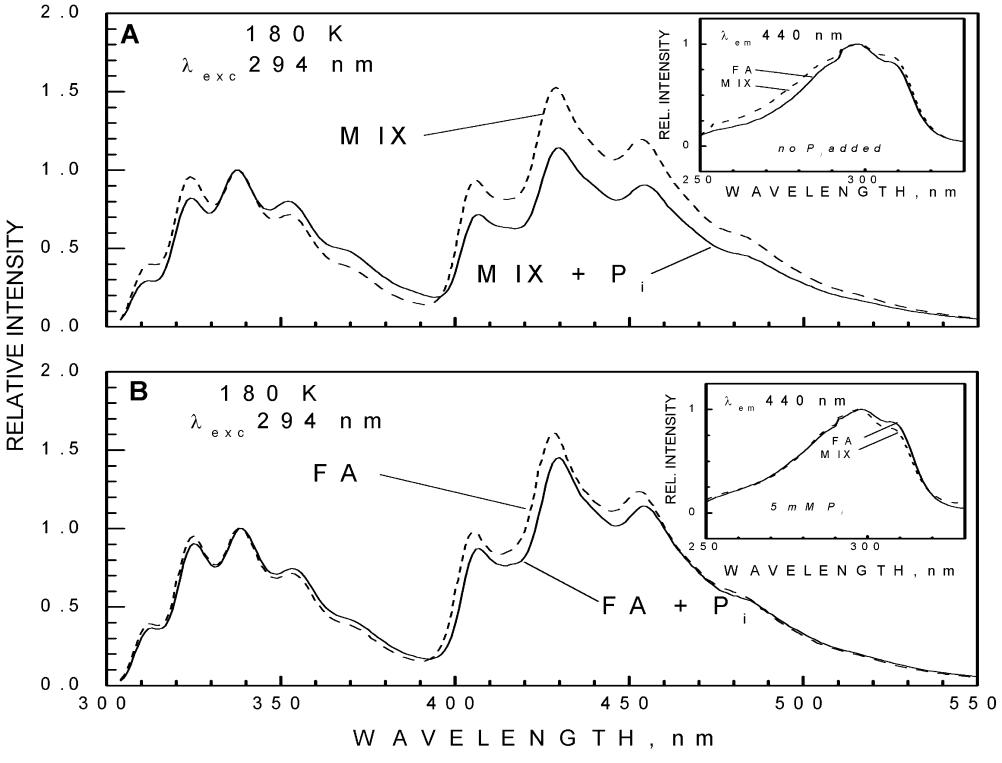

Fig. 5 Fluorescence and phosphorescence emission spectra ($\lambda_{exc} = 294$ nm) of (**A**) a mixture of 1 μM PNP and 25 μM FA and (**B**) 25 μM FA, in 50 mM Hepes (pH 7) containing 80% glycerol at 180 K, in the absence (*dashed line*) and presence (*full line*) of 5 mM P_i. The *inset* show the phosphorescence excitation spectra ($\lambda_{em} = 440$ nm) of 25 μM FA (*full line*) and its mixture with 1 μM PNP (*dashed line*) in the absence (*upper frame*) and presence (*lower frame*) of 5 mM P_i. The maximum intensities of the fluorescence emission are normalized to unity

enzyme and ligand. They reflect the simultaneous occurrence of the following phenomena:

1. Partial quenching of intrinsic tyrosine fluorescence of the enzyme mainly by FRET from tyrosine residue(s) to the base moiety of FA. Examination of the crystal structures of *E. coli* PNP (Mao et al. 1997) and its complex with FB (Koellner et al. 1998) and m^6FA (Koellner et al. 2002) suggest that the most probable candidate for the donor is Tyr160, involved in the π–π staking interactions with FB or m^6FA, widely observed in other protein–ligand systems (McGaughey et al. 1998; Burley and Petsko 1985). Therefore, higher order multipole couplings as well as exchange interactions between donor and acceptor must be included in further studies. At this moment, it is hard to conclude if the long-distance dipole–dipole interactions should be omitted, since there are also several Tyr residues in the range of 12–24 Å from the ligand base moieties (Koellner et al. 1998, 2002), which can be considered as potential energy donors.
2. Enhancement of the protein fluorescence quenching by addition of the second ligand P_i (substrate), based of the effect of P_i on the emission properties of the complex. These effects reflect changes in polarity in the ligand-binding pocket induced by the negatively charged phosphate anion, similar to the previously observed shift of the population of the N(2)–H form from 15% in FA to as much as 50% in FA-5′-phosphate, depending on whether the phosphate moiety is in the monoanionic or dianionic form (Wierzchowski et al. 1984).
3. A shift in the tautomeric equilibrium of FA towards the N(2)–H form, which is preferentially bound by the enzyme. This is shown by comparison of the fluorescence and phosphorescence properties of bound FA with that of the free nucleoside and of chemical models of the fixed N(1)–H and N(2)–H tautomers, i.e. m^1FA and m^2FA (Wierzchowski and Shugar 1982).

The results presented here remove ambiguities found in X-ray crystallographic studies of the crystal structure of the active center of *E. coli* PNP in a complex with FB (Koellner et al. 1998), because the crystal data could not distinguish between two possible hydrogen bonds between FB and the protein, one from the ring N(1) to the O^{δ} of Asp204, the other from N(1) to the O^{γ} of Ser90. Involvement of the N(2)–H of FA in the complex formation with *E. coli* PNP implies that N(1) [corresponding to N(7) in purine nucleosides] is a proton acceptor in a hydrogen bond with Asp204, which should then exist in the protonated form in the complex. Consistent with this, the ring N(2) is a proton donor in the second hydrogen bond to the O^{γ} of Ser90. This is an additional hydrogen bond, which is not present in complexes with purine nucleosides, where the ring C(8) corresponds to the N(2) of FA. Consistent with this is the fact that substitution of C(8) by an amino group (proton donor) led to enhanced affinity of the 8-amino analogues to the enzyme (Pugmire and Ealick 2002).

The aforementioned is highly relevant to the molecular mechanism of action of *E. coli* PNP as well as PNP from mammalian sources. Most important is the possible existence of Asp204 in the protonated form in the complex, which may be critical for transition state stabilization, as was postulated for the human enzyme where an analogous role was suggested for Asn243 (Erion et al. 1997a, 1997b). This is in line with the fact that replacement of Asn243 by Ala abolished activity versus Ino and Guo, and substitution by Asp modified the substrate specificity of the human enzyme such that it resembled that of *E. coli* PNP (Stoeckler et al. 1997).

Acknowledgements This research was supported by the State Committee for Scientific Research (KBN), which includes 3P04A02425, BW-1565/BF and BST-718/BF.

References

Ames BN (1966) Assay of inorganic phosphate. Methods Enzymol 8:115–116

Bezirjian KhO, Kocharian ShM, Akopyan ZhI (1986) Isolation of hexameric form of purine nucleoside phosphorylase from *E. coli*. Comparative study of trimeric and hexameric form of the enzyme. Biokhimia 51:1085–1092

Burley SK, Petsko GA (1985) Aromatic–aromatic interactions: a mechanism of protein structure stabilization. Science 229:23–28

Buxton RS, Hammer-Jespersen K, Valentin-Hansen P (1980) A second purine nucleoside phosphorylase in *Escherichia coli* K-12. I. Xanthosine phosphorylase regulatory mutants isolated as secondary-site revertants of a *deoD* mutant. Mol Gen Genet 179:331–340

Bzowska A, Kulikowska E, Shugar D (1992) Formycins A and B and some analogues: selective inhibitors of bacterial (*Escherichia coli*) purine nucleoside phosphorylase. Biochim Biophys Acta 1120:239–247

Bzowska A, Kulikowska E, Shugar D (2000) Purine nucleoside phosphorylases: properties, functions, and clinical aspects. Pharmacol Ther 88:349–425

Chenon MT, Panzica RP, Smith JC, Pugmire RJ, Grant DM, Townsend LB (1976) Carbon-13 magnetic spectra of C-nucleosides. 3. Tautomerism in formycin and formycin B and certain pyrazolo[4,3-*d*]pyrimidines. J Am Chem Soc 98:4736–4745

Dawson RMC, Elliott DC, Elliott WH, Jones KM (eds) (1969) Spectral data and p*K* values for purines, pyrimidines, nucleosides and nucleotides. In: Data for Biochemical Research. Oxford University Press, Oxford, p 176

Doskocil J, Holy A (1977) Specificity of purine nucleoside phosphorylase from *Escherichia coli*. Collect Czech Chem Commun 42:370–383

Eftink MR (1997) Fluorescence methods for studying equilibrium macromolecule–ligand interactions. Methods Enzymol 278:221–257

Erion MD, Stoeckler JD, Guida WC, Walter RL, Ealick SE (1997a) Purine nucleoside phosphorylase. 2. Catalytic mechanism. Biochemistry 36:11735–11748

Erion MD, Takabayashi K, Smith HB, Kessi J, Wagner S, Honger S, Shames SL, Ealick SE (1997b) Purine nucleoside phosphorylase. 1. Structure–function studies. Biochemistry 36:11725–11734

Förster Th (1948) Intermolecular energy migration and fluorescence. Ann Phys (Leipzig) 2:55–75

Gilbertsen RB, Sircar JC (1990) Enzyme cascades: purine metabolism and immunosuppression. In: Hansch C, Sammes PG, Taylor JB (eds) Comprehensive medicinal chemistry, vol 2. Pergamon Press, Oxford, p 443

Giziewicz J, Shugar D (1977) Preparation and properties of formycin analogues methylated on the pyrazole ring nitrogens and/or the ribose *cis* hydroxyls. Acta Biochim Polon 24:231–246

Halazy S, Ehrhard A, Danzin C (1991) 9-(Difluorophosphonoalkyl)-guanines as a new class of multisubstrate analogue inhibitors of purine nucleoside phosphorylase. J Am Chem Soc 113:315–317

Hammer-Jespersen K, Buxton RS, Hansen TD (1980) A second purine nucleoside phosphorylase in *Escherichia coli* K-12. II. Properties of xanthosine phosphorylase and its induction by xanthosine. Mol Gen Genet 179:341–348

Hirshfield MS, Chaffe S, Koro-Johnson L, Mary A, Smith AA, Short SA (1991) Use of site-directed mutagenesis to enhance the epitope-shielding effect of covalent modification of proteins with polyethylene glycol. Proc Natl Acad Sci USA 88:7185–7189

Hughes BW, Wells AH, Bebok Z, Gadi VK, Garver RI Jr, Parker WB, Sorscher EJ (1995) Bystander killing of melanoma cells using the human tyrosinase promoter to express the *Escherichia coli* purine nucleoside phosphorylase. Cancer Res 55:3339–3345

Jensen KF (1976) Purine nucleoside phosphorylase from *Salmonella typhimurium* and *Escherichia coli*. Eur J Biochem 61:377–386

Jensen KF, Nygaard P (1975) Purine nucleoside phosphorylase from *Escherichia coli* and *Salmonella typhimurium*. Purification and some properties. Eur J Biochem 51:253–265

Kalckar HM (1947) The enzymatic synthesis of purine-ribosides. J Biol Chem 167:429–443

Kierdaszuk B (2002) Emission spectroscopy of complex formation between *Escherichia coli* purine nucleoside phosphorylase (PNP) and identified tautomeric species of formycin inhibitors resolves ambiguities found in crystallographic studies. In: Kraayenhof R, Visser AJWG, Gerritsen HC (eds) Fluorescence spectroscopy, imaging and probes. New tools in chemical, physical and life sciences. (Springer series on fluorescence, vol. 2) Springer, Heidelberg, pp 277–296

Kierdaszuk B, Modrak-Wójcik A, Shugar D (1997) Binding of phosphate and sulfate anions by purine nucleoside phosphorylase from *E. coli*: ligand dependent quenching of enzyme intrinsic fluorescence. Biophys Chem 63:107–118

Kierdaszuk B, Modrak-Wójcik A, Wierzchowski J, Shugar D (2000) Formycin A and its N-methyl analogues, specific inhibitors of *E. coli* purine nucleoside phosphorylase (PNP): induced tautomeric shifts on binding to enzyme, and enzyme → ligand fluorescence resonance energy transfer. Biochim Biophys Acta 1476:109–128

Koellner G, Luić M, Shugar D, Saenger W, Bzowska A (1998) Crystal structure of the ternary complex of *E. coli* purine nucleoside phosphorylase with formycin B, a structural analogue of the substrate inosine, and phosphate (sulphate) at 2.1 Å resolution. J Mol Biol 280:153–166

Koellner G, Bzowska A, Wielgus-Kutrowska B, Luic M, Steiner T, Saenger W, Stepinski J (2002) Open and closed conformation of the *E. coli* purine nucleoside phosphorylase active center and implications for the catalytic mechanism. J Mol Biol 315:351–71

Koszalka GW, Vanhooke J, Short SA, Hall WW (1988) Purification and properties of inosine-guanosine phosphorylase from *Escherichia coli* K-12. J Bacteriol 170:3493–3498

Kredich NM, Hershfield MS (1989) Immunodeficiency diseases caused by ADA deficiency and PNP deficiency. In: Jeffers JD, Gavret G (eds) The metabolic basis of inherited diseases. McGraw-Hill, New York, pp 1045–1075

Krenitsky TA, Tuttle JV, Miller WH, Moorman AR, Orr GF, Beauchamp L (1990) Nucleotide analogue inhibitors of purine nucleoside phosphorylase. J Biol Chem 265:3066–3069

Lakowicz JR (1999) Principles of fluorescence spectroscopy. Plenum, New York, pp 44–47, 211–214, 439–440

Lister JH (1971) In: Brown DJ (ed) Fused pyrimidines, part II: purines. Wiley, New York

Mao C, Cook WJ, Zhou M, Koszalka G, Krenitsky TA, Ealick SE (1997) The crystal structure of *E. coli* purine nucleoside phosphorylase: a comparison with human enzyme reveals a conserved topology. Structure 5:1373–1383

McGaughey GB, Gagne M, Rappe AK (1998) Stacking interactions. Alive and well in proteins. J Biol Chem 273:15458–15463

Montgomery JA (1993) Purine nucleoside phosphorylase: a target for drug design. Med Res Rev 13:209–228

Parker CA (1968) Photoluminescence of solutions. Elsevier, Amsterdam, pp 272–275

Psoda A, Shugar D (1971) Spectral studies on tautomeric forms of inosine. Biochim Biophys Acta 247:507–513

Pugmire MJ, Ealick SE (2002) Structural analyses reveal two distinct families of nucleoside phosphorylases. Biochem J 361:1–25

Sorscher EJ, Peng S, Bebok Z, Allan PW, Bennrtt LL Jr, Parker WB (1994) Tumor cell bystander killing in colonic carcinoma utilizing the *Escherichia coli* DeoD gene to generate toxic purines. Gene Therapy 1:233–238

Stoeckler JD (1984) Purine nucleoside phosphorylase: a target for chemotherapy. In: Glazer RI (ed) Developments in cancer chemotherapy. CRC Press, Boca Raton, Fla., pp 35–60

Stoeckler JD, Agarwal RP, Agarwal KC, Parks RE Jr (1978) Purine nucleoside phosphorylase from human erythrocytes. Methods Enzymol 51:530–538

Stoeckler JD, Cambor C, Burgess FW, Erban SB, Parks RE Jr (1980) Purine nucleoside phosphorylase inhibitors as potential chemotherapeutic and immunosuppressive agents. Pharmacologist 22:99–105

Stoeckler JD, Poirot AF, Smith RM, Parks RE Jr, Ealick SE, Takabayashi K, Erion MD (1997) Purine nucleoside phosphorylase. 3. Reversal of purine base specificity by site-directed mutagenesis. Biochemistry 36:11749–11756

Stoychev G, Kiedaszuk B, Shugar D (2001) Interaction of *Escherichia coli* purine nucleoside phosphorylase (PNP) with the cationic and zwitterionic forms of the fluorescent substrate N(7)-methylguanosine. Biochim Biophys Acta 1544:74–88

Tuttle JV, Krenitsky TA (1984) Effects of acyclovir and its metabolites on purine nucleoside phosphorylase. J Biol Chem 259:4065–4069

Ward DC, Reich E, Stryer L (1969) Fluorescence studies of nucleotides and polynucleotides. I. Formycin, 2-aminopurine riboside, 2,6-diaminopurine riboside, and their derivatives. J Biol Chem 244:1228–1237

Wierzchowski J, Shugar D (1982) Luminescence studies of formycin, its aglycone, and their N-methyl derivatives: tautomerisation, sites of protonation and phototautomerism. Photochem Photobiol 35:445–458

Wierzchowski J, Shugar D (1993) Amino–imino tautomerism of N(6)-methylformycin, a potent inhibitor of *E. coli*, but not mammalian, purine nucleoside phosphorylase. Collect Czech Chem Commun 58:14–17

Wierzchowski J, Kuśmierek J, Giziewicz J, Salvi D, Shugar D (1980) Analogues of formycin A and B: synthesis and some properties of methyl derivatives of 7-amino- and 7-ketopyrazolo[4,3-*d*]pyrimidines. Acta Biochim Polon 27:35–56

Wierzchowski J, Lassota P, Shugar D (1984) Continuous fluorimetric assay of 5′-nucleotidase with 5′-formycin phosphate as substrate, and its application to properties of substrates and inhibitors. Biochim Biophys Acta 786:170–178

Wierzchowski J, Wielgus-Kutrowska B, Shugar D (1996) Fluorescence emission properties of 8-azapurines and their nucleosides, and application to the kinetic of the reverse synthetic reaction of purine nucleoside phosphorylase. Biochim Biophys Acta 1290:9–17

Wu P, Brand L (1994) Resonance energy transfer: methods and applications. Anal Chem 218:1–13